Effect of yttrium addition on water-gas shift reaction over CuO/CeO2 catalysts

ARTICLE *in* JOURNAL OF RARE EARTHS · JUNE 2009

Impact Factor: 1.26 · DOI: 10.1016/S1002-0721(08)60262-8

6 AUTHORS, INCLUDING:

Lei Li
Jiaxing University
26 PUBLICATIONS **248** CITATIONS
SEE PROFILE

Yingying Zhan
Fuzhou University
38 PUBLICATIONS **1,529** CITATIONS
SEE PROFILE

Available online at www.sciencedirect.com
ScienceDirect
JOURNAL OF RARE EARTHS
www.re-journal.com/en/
JOURNAL OF RARE EARTHS, Vol. 27, No. 3, Jun. 2009, p. 411

Effect of yttrium addition on water-gas shift reaction over CuO/CeO_2 catalysts

SHE Yusheng (佘育生), LI Lei (李 雷), ZHAN Yingying (詹瑛瑛), LIN Xingyi (林性贻), ZHENG Qi (郑 起), WEI Kemei (魏可镁)

(National Engineering Research Center of Chemical Fertilizer Catalysts, Fuzhou University, Fuzhou 350002, China)

Received 3 September 2008; revised 24 November 2008

Abstract: This paper presented a study on the role of yttrium addition to CuO/CeO_2 catalyst for water-gas shift reaction. A single-step co-precipitation method was used for preparation of a series of yttrium doped CuO/CeO_2 catalysts with yttrium content in the range of 0–5wt.%. Properties of the obtained samples were characterized and analyzed by X-ray diffraction (XRD), Raman spectroscopy, H_2-TPR, cyclic voltammetry (CV) and the BET method. The results revealed that catalytic activity was increased with the yttrium content at first, but then decreased with the further increase of yttrium content. Herein, CuO/CeO_2 catalyst doped with 2wt.% of yttrium showed the highest catalytic activity (CO conversion reaches 93.4% at 250 °C) and thermal stability for WGS reaction. The catalytic activity was correlated with the surface area, the area of peak γ of H_2-TPR profile (i.e., the reduction of surface copper oxide (crystalline forms) interacted with surface oxygen vacancies on ceria), and the area of peak C_2 and A_1 ($Cu^0 \leftrightarrow Cu^{2+}$ in cyclic voltammetry process), respectively. Besides, Raman spectra provided evidences for a synergistic Cu-$O_{vacancy}$ interaction, and it was indicated that doping yttrium may facilitate the formation of oxygen vacancies on ceria.

Keywords: CuO/CeO_2 catalyst; water-gas shift; yttrium; cyclic voltammetry; rare earths

The water-gas shift reaction (WGSR), $CO+H_2O \leftrightarrow CO_2+H_2$, has been applied as an important industrial process for hydrogen production in synthesis of ammonia and adjusting the CO/H_2 ratio for subsequent synthesis of methanol. Recently, low-temperature WGSR has attracted renewed interest due to the increasing demands for high-purity hydrogen for application in fuel-cell systems[1]. As we know, removal of carbon monoxide (CO) in the hydrogen fuel produced by reforming of hydrocarbon sources is indispensable to attain high and stable performances of polymer electrolyte fuel cells (PEFCs) because CO is irreversibly adsorbed on the platinum electrode of a PEFC. The WGSR has been used in industry to achieve the removal of CO in the relatively high concentration range (ca.7%–10%CO), with the help of effective catalyst systems abreast of the harsher reaction conditions[2]. It has been reported that the supported precious metal catalysts, such as Au/CeO_2[3], Au/TiO_2[4], Au/Fe_2O_3[5], Pd/CeO_2[6], Pt/Al_2O_3[7], Pt/CeO_2[8], Rh/Fe_2O_3[9] and so on, showed high catalytic activity for the reaction. However, considering the high cost of the above precious metals or their instability, more and more researchers have given their attentions to the base metal catalysts including copper.

Many studies[10–12] have shown that ceria-supported copper catalysts exhibit highly activity for the WGS reaction. Li et al.[10] recently reported that Cu-loaded ceria catalyst (especially 5% Cu-Ce $(La)O_x$) retained highly catalytic activity for the WGS reaction even at 600 °C, with the feed gas only containing CO, H_2O and inert gas. In order to apply these catalysts in fuel-cell power generation, Qi et al.[12] investigated the effect of H_2 and CO_2 on the activity and stability of $Cu-CeO_2$ catalysts, finding that both activity and stability of such catalysts were decreased when H_2 and CO_2 were added. Therefore, it is challenge work to search a suitable catalyst for WGS reaction in the presence of H_2 and CO_2.

Yttrium is an element that has been often doped into CeO_2 materials. As a dopant, yttrium can improve the thermal stability and anti-aging performance of CeO_2 materials[13]. Y-doped CeO_2 has relatively high electrical conductivity in all doped CeO_2 materials, although the association enthalpy between dopant cation and oxygen vacancy is a little large[14,15]. Furthermore, as yttrium resource is in abundance, the Y-doped materials have attracted more and more special interests in many fields. Before 2000, there was little

Foundation item: Project supported by the National Natural Science Foundation of China (20771025) and A-type Science and Technology Projects of Fujian Provincial Department of Education (JA08021)

Corresponding author: ZHENG Qi (**E-mail:** qizheng2005@gmail.com)

DOI: 10.1016/S1002-0721(08)60262-8

research in nanosized CeO_2 doped with rare earth elements. With the rapid development of economy and a requirement for new materials, there are more efforts focused on the preparation, performance and application of CeO_2 material doped with rare-earth elements including yttrium[16–18]. Whereas, no work regarding the catalysts of copper oxide supported yttrium-doped ceria for WGS reaction has been reported.

In this work, yttrium was first introduced to CuO/CeO_2 catalyst, with a co-precipitation method, to modify its activity and stability. The correlation of catalyst structure and catalytic performance was investigated by XRD, BET, Raman spectroscopy, H_2-TPR and CV techniques. The results suggested that only small doping (ca. 1wt.%–2wt.%) of yttrium increased the number of active site (i.e., the copper species interacted with surface oxygen vacancies on ceria) for WGS reaction and subsequently showed the highest catalytic activity.

1 Experimental

1.1 Catalysts preparation

A series of yttrium doped CuO/CeO_2 catalysts with fixed copper content (25wt.%, calculated as CuO) and a given yttrium content (e.g., 0wt.%, 1wt.%, 2wt.%, 3wt.%, 5wt.%, calculated as Y_2O_3) were prepared by parallel co-precipitation method. The obtained samples were denoted as CCY0, CCY1, CCY3 and CCY5, respectively. Stoichiometric amounts of $Cu(NO_3)_2{\cdot}3H_2O$, $Ce(NO_3)_3{\cdot}6H_2O$ and $Y(NO_3)_3{\cdot}9H_2O$ were first dissolved in deionized water, then the mixed aqueous solution were co-precipitated with an aqueous solution of KOH under vigorous stirring at T=80 °C and pH=10±1. A black suspension was acquired and aged with continuous stirring at 80 °C for 6 h. The resulting precipitate was centrifuged and washed by deionized water for several times, then dried at 120 °C for 12 h and finally calcined at 650 °C for 4 h (heating rate was 5 °C/min) in air.

1.2 Characterization

Power XRD patterns of the as-synthesized samples were recorded on a PANalytical X' pert Pro diffractometer with an X' Celerator detector, operating at 40 kV and 40 mA, using Co Kα radiation (l=0.17902 nm). The crystal size of ceria and copper oxide was determined from the peak broadening with the Scherrer equation.

The BET surface area and pore volume were measured on a Micromeritics ASAP 2020 physical adsorption analyzer, at –196 °C using nitrogen as adsorbate. Prior to each analysis, the sample was degassed at 200 °C for 3 h to obtain a residual pressure of less than 1×10^{-5} Torr.

Raman spectra were collected at room temperature on a Renishaw Invia Plus system. The samples were excited with a 514.5 nm laser line.

Temperature-programmed reduction (TPR) measurement was carried out on an AutoChem 2910 instrument. The H_2-TPR was performed by passing 10% H_2/Ar (flowing rate= 30 ml/min) on 50 mg catalyst at a heating rate of 10 °C/min. Prior to TPR, the samples were pretreated under Argon atmosphere at 200 °C for 30 min. Then the system was cooled to ambient temperature under a pure Argon gas. The hydrogen consumption was monitored by a thermal conductivity detector (TCD).

The cyclic voltammetry (CV) spectra were recorded at ambient temperature by a CHI 614B potentiostat/galvanostat with three-electrode cell configuration. 5 mg of catalysts and 1 mg of carbon black (Vulcan XC-72R) were suspended in 1 ml of ethanol and 15 μl of Nafion solution to prepare catalyst ink. Then 25 μl of ink was transferred with an injector to clean glassy carbon disk electrode. After the ethanol volatilization, the electrode was heated at 75 °C for 5 min. Sodium sulfate (0.05 mol/L) was used as the electrolyte solution. The counter and reference electrodes are Pt foil and $Hg/Hg_2SO_4/H_2SO_4$ (0.5 mol/L), respectively. Prior to the measurement, the electrolyte solution was degassed by bubbling with high pure nitrogen (99.999%). The electrodes were cycled from +0.8 to –1.6 V at a scan rate of 10 mV/s.

1.3 Evaluation of catalytic performance

The catalytic activities and thermal stabilities of the catalysts for WGS reaction were tested in a fixed bed reactor at atmospheric pressure. 2 g of catalysts (30–40 mesh) was placed between two layers of quartz granules inside a stainless steel tube (i.d.=12 mm). The experiment was directly performed under a feed gas (10% CO, 60% H_2, 12% CO_2 and balance N_2) flowing at 103.7 ml/min without pre-reduction. The ratio of vapor to feed gas was maintained at 1:1. The residual water of the outlet was removed by a condenser before entering a gas chromatograph (102G) equipped with a thermal conductivity detector (TCD). The activity was expressed by the conversion of CO, defined as: $X_{CO}(\%)=(1-V'_{CO}/V_{CO})\times100\%/(1+V'_{CO})$, where V_{CO} and V'_{CO} are the inlet and outlet content of CO, respectively. The catalytic activity was first measured from 200 to 400 °C, then kept at 400 °C for 10 h and decreased to 200 °C, and finally increased to 400 °C again to investigate the thermal stability of the catalysts.

2 Results and discussion

2.1 Catalytic performance of Y-doped CuO/CeO_2 catalyst

Fig.1 shows the WGS activities of yttrium doped CuO/CeO_2 catalysts. The CO conversion is increased with the yttrium content at first (from CCY0 to CCY2), but then decreased with the further increase of yttrium content. The CO conversion reaches the maximum at CCY2, with the value of 93.4% at 250 °C, which is an increment of 8.1% compared with that of CCY0 (86.4%).

Fig.2 shows the thermal stabilities of yttrium doped CuO/CeO_2 catalysts at 250 °C for WGS reaction. As seen in Fig.2, the CO conversion of CCY2 is decreased from 93.4% to 89.9%, corresponding to the relative deactivation of 3.9%, which is much smaller than that of CCY0 and CCY5. It suggests that the addition of proper quantity of yttrium can effectively enhance thermal stability of CuO/CeO_2 catalysts.

2.2 Structural studies of Y-doped CuO/CeO_2 catalysts

Fig.3 shows the XRD patterns of the prepared samples.

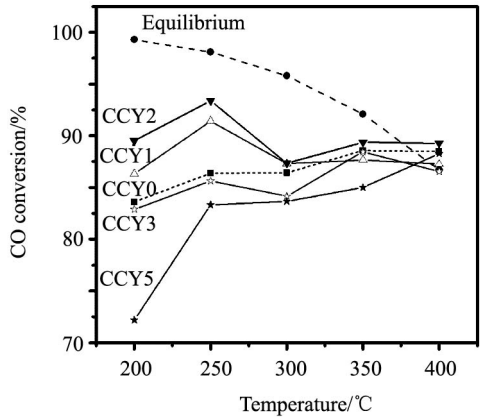

Fig.1 WGS activities of the yttrium doped CuO/CeO_2 catalysts (feed gas: 10% CO, 60% H_2, 12% CO_2 and balance N_2; Vapor-gas: 1:1 (mol); W/F=1.54 g s/cm^3)

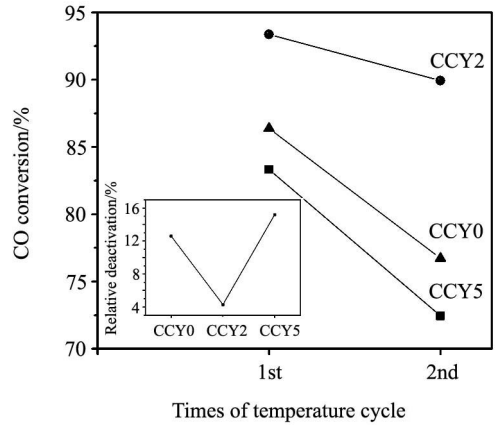

Fig. 2 Thermal stabilities of yttrium doped CuO/CeO_2 catalysts after keeping at 400 °C for 10 h (inset: relative deactivation of catalysts at 250 °C)

(comparison of catalytic activity at 250 °C between the first and the second cycle)

The distinct fluorite oxide diffraction pattern of CeO_2 and the strong diffraction peaks of CuO are detected in all of the samples. No obvious diffraction lines, ascribed to yttrium or its derivates, are detected, which indicates that yttrium might enter the CeO_2 frame or was highly dispersed in the catalysts. With the increase of yttrium content, the cell parameter of CeO_2 (111) is almost identical, indicating that the doping yttrium was highly dispersed in the catalysts rather than entering the CeO_2 frame. As the doping concentration of yttrium increases, the crystal size of CeO_2 (111) is decreased gradually (from 10.3 nm to 7.9 nm, see Table 1), corresponding to the broadening of diffraction peaks of CeO_2. However, the change of crystal size of CuO in CCY0–CCY5 samples is not distinct.

Xie et al.[19] reported the spontaneous monolayer dispersion principle that many oxides and salts can disperse spontaneously onto the surface of supports to form a monolayer or submonolayer. Chen et al.[20] calculated the dispersion threshold of many oxides and salts on the supports with the "Incorporation Model". The results indicate that the dispersion threshold of yttrium on the ceria is 0.0622 g/100 m^2. Similarly, the dispersion threshold of yttrium on the as-synthesized catalysts is about 0.0286 g/1 g (i.e., 2.86wt.%). The reason for the decrease of the crystal size might be ascribed to that the doping yttrium, dispersed spontaneously onto the surface of the supports to form the monolayer or sub-monolayer, prevents the agglomeration of copper oxide and ceria. On the other hand, the lattice strain of CeO_2 (111) increased obviously with the increase of yttrium content, while the variation of lattice strain of CuO is minor and neglectable, indicating that the doping yttrium exhibits larger effect on the CeO_2 than the CuO. This suggests that the yttrium is dispersed primarily onto the surface of CeO_2 rather than that of CuO.

The texture properties of the catalysts are listed in Table 1. BET surface area of fresh catalysts varied with the yttrium content, and reached the maximum at CCY2 (53 m^2/g), which is an increment of 26.2% compared with that of CCY0

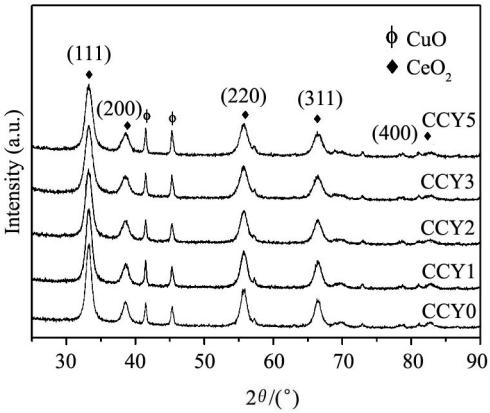

Fig.3 XRD patterns of yttrium doped CuO/CeO_2 catalysts

Table 1 BET surface area, pore parameter, crystal size, lattice parameter of as-synthesized catalysts*

Catalysts	S_{BET}/(m^2/g)		Pore volume/	Crystal size/nm[b]		Cell parameter/nm[c]	Lattice strain/%[d]	
	Fresh	Used[a]	(ml/g)	CeO_2(111)	CuO(111)	a_{CeO2}	CeO_2(111)	CuO(111)
CCY0	42	33	0.25	10.3	29.3	0.5420	1.361	0.327
CCY1	50	38	0.30	9.6	31.5	0.5420	1.466	0.253
CCY2	53	42	0.25	8.7	27.7	0.5418	1.640	0.360
CCY3	46	35	0.26	7.8	30.2	0.5423	1.811	0.317
CCY5	39	29	0.25	7.9	34.1	0.5424	1.812	0.291

* a: the catalysts underwent the activities and thermal stabilities test and were cooled to ambient temperature without feed gas; b: calculated from the peak at 33.2°, 41.5° for CeO_2 (111), CuO (111) by the Scherrer equation, respectively; c: calculated from the peak at 33.2° by $d^2=a^2/(H^2+K^2+L^2)$ equation depended on d- spacing; d: calculated from the peak at 33.2°, 41.5° for CeO_2 (111), CuO (111)

(42 m^2/g). The larger surface area of CCY1 and CCY2 might be attributed to that the appropriate amount (smaller than the dispersion threshold) of yttrium, dispersed spontaneously onto the surface of CeO_2, prevents the agglomeration of copper oxide and ceria. It is found that the variation of surface area shows the same trend as that of catalytic activity, indicating that the surface area has large effect on the catalytic performance in the present case. Besides, the surface area of used catalysts is smaller than that of the fresh ones (e.g., 34.5% for CCY5), which suggests that the increase of particle size during the activity evaluation leads to the deactivation of the catalysts.

Compared with XRD results which yield information related to the cation sublattice, Raman spectroscopy of these fluorite type oxide structures is dominated by oxygen lattice vibrations.

The visible Raman spectra between pure and Y-doped CuO/CeO_2 catalysts are shown in Fig.4. A sharp peak at about 450 cm^{-1} ascribed to cubic CeO_2 is observed in all cases. It is noted that this peak is shifted significantly to lower wavenumber when the yttria is added as dopant. Most previous works interpret this shifting as the presence of oxygen vacancies[21], which was correlated with changes of

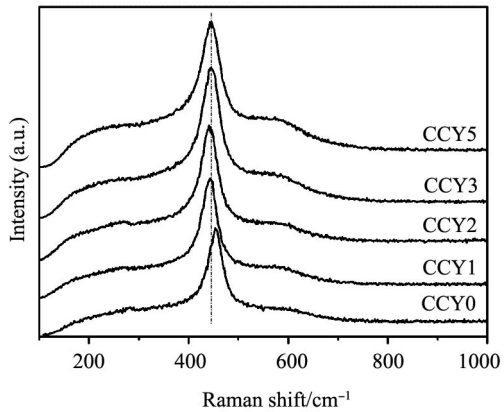

Fig.4 Raman spectra of Y-doped CuO/CeO_2 catalysts excited by 514.5 nm laser line

CeO_2 environment in the presence of copper and yttrium. It also means that the probable enhancement of interaction between Cu ions and Ceria oxide occurs. In addition, the relative intensity of a broad band covering from 500 and 650 cm^{-1}, which has been also related to the occurrence of oxygen vacancies[22], is increased with increasing the amount of yttrium introduced, indicating the increasing number of oxygen vacancies. Thus, it is concluded that the doping of yttrium promotes the formation of oxygen vacancies on ceria, and effectively enhances the interaction between copper and ceria oxide.

2.3 Redox properties of Y-doped CuO/CeO_2 catalysts

Fig.5 shows the H_2-TPR profiles of the CuO/CeO_2 catalysts with different dopant content. All the curves are fitted into four peaks with Gauss-Lorentz method as those in Ref.[23]. The peak positions and their contributions are

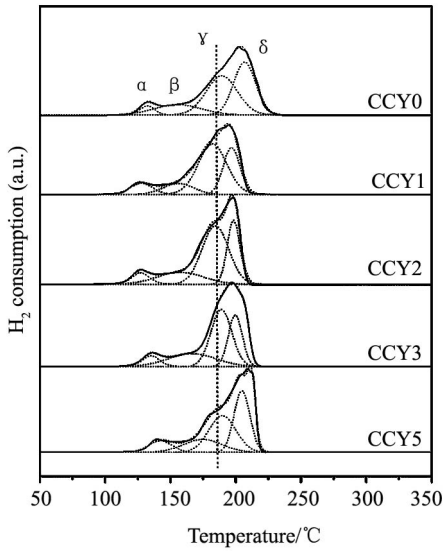

Fig.5 H_2-TPR profiles of the yttrium doped CuO/CeO_2 catalysts (solid lines are experimental curves and dot lines are Gauss-Lorentz fitted curves)

summarized in Table 2. According to literatures[24–26], the peaks α and β are attributed to the reduction of non-crystalline copper oxide strongly interacting with CeO_2 and that of larger copper oxide particles weakly associated with CeO_2, respectively. The peak γ is ascribed to the reduction of surface copper oxide (crystalline forms) which interacted with surface oxygen vacancies on ceria. The peak δ is due to the reduction of pure bulk crystalline copper oxide, which does not associate with CeO_2.

It is noted that, compared with CCY0, the addition of yttrium leads to a slight shift of the peaks to lower temperature, which could be related to the presence of highly dispersable and more easily reducible CuO species, indicating that the presence of dopant enhances the reduction properties of CuO/CeO_2. Moreover, the reduction temperature of CCY1 and CCY2 samples with high activity was lower than that of other samples. It might mean that the high reducibility of CuO is required as the catalysts show high activity. However, the order of the reducibility of these samples does not completely agree with that of the catalytic activities of these samples, suggesting that not only the reducibility of CuO but also the other interaction between copper oxide and support should be considered to explain the catalytic performances of the Cu/CeO_2 catalysts.

Interestingly, among all these samples, the area of peak α and β does not differ very much, while the area of peak γ increases with the content of yttria, reaching the maximum at CCY2, then decreases at CCY3 and CCY5 compared with CCY0. As the yttria content is less than the dispersion threshold (2.86wt.%) of the yttria on the ceria, the doping yttria is dispersed spontaneously onto the surface of CeO_2 to form the monolayer, and prevents copper oxide and ceria from agglomeration and improves the mutual dispersion degree between the crystal CuO and ceria, resulting in the increase of the crystal CuO interacted with the surface oxygen vacancies on ceria. Thus the area of peak γ reaches the maximum at CCY2. While the decreasing area of peak γ at CCY3 and CCY5 might be attributed to that the excess yttria is still dispersed spontaneously onto the surface of the crystal CuO and prevents the interaction between CuO and the surface oxygen vacancies on ceria. Correlated to the catalytic activities, it is obviously observed that the variation of peak γ′ area is well consistent with that of catalytic activity, indicating that the area of peak γ has large effect on the catalytic activity. In other words, the catalytic activity might be mainly affected by the number of reducible surface copper oxide (crystalline forms) which interacted with surface oxygen vacancies on ceria.

Table 2 H_2-TPR peak positions and concentrations of reducible species in yttrium doped CuO/CeO_2 catalysts as determined by the Gauss-Lorentz fit of TPR profiles

Catalysts	TPR peak position (temperature/℃) and area (a.u.)*			
	Peak α	Peak β	Peak γ	Peak δ
CCY0	132.3 (0.31)	155.5 (1.15)	189.4 (2.97)	206.9 (2.85)
CCY1	127.9 (0.61)	156.2 (0.81)	182.3 (3.61)	196.8 (1.92)
CCY2	127.8 (0.56)	154.9 (1.36)	182.9 (3.84)	198.2 (1.99)
CCY3	128.8 (0.62)	172.3 (1.47)	189.2 (2.93)	199.4 (2.02)
CCY5	142.3 (0.65)	174.9 (1.20)	189.8 (2.43)	204.4 (2.38)

* Values in parentheses are the area of each peaks calculated by fitted result

Moreover, considering cyclic voltammetry test can provide convincing evidences for the redox ability of redox couples during the oxidation and reduction procedures[27], in this work, the redox abilities of Y-doped CuO/CeO_2 catalysts and their effects on the catalytic performances are further investigated with the aid of CV technique, which is a potential tool to study catalytic reaction not only in homogeneous catalysis but also in heterogeneous catalysis[28].

Fig.6 shows the cyclic voltammograms of copper species in yttrium doped CuO/CeO_2 catalysts. The voltammograms consist of two cathodic (peak C_1 and C_2) and two anodic (peak A_1 and A_2) peaks in the scan range of +0.8 to –1.6 V vs. $Hg/Hg_2SO_4/H_2SO_4$ (0.5 mol/L). In order to designate the peaks, the first step in the interpretation of cyclic voltammograms is the calculation of the thermodynamic reversible potentials of all the possible reactions. The standard potential can be calculated as $E^0=-\Delta G^0/nF$. In the case of copper oxides, some possible reactions are:

$$2CuO+2H^++2e=Cu_2O+H_2O \quad (1)$$

E^0=0.64 V vs. SHE; at pH 7, E_{rev}=0.23 V vs. SHE

$$Cu_2O+2H^++2e=2Cu+H_2O \quad (2)$$

E^0=0.47 V vs. SHE; at pH 7, E_{rev}=0.06 V vs. SHE

$$CuO+2H^++2e=Cu+H_2O \quad (3)$$

E^0=0.56 V vs. SHE; at pH 7, E_{rev}=0.15 V vs. SHE

where the E_{rev} is calculated as $E_{rev}=E^0+RT/nF$ ln ([Ox]/[Red]) (Nernst's equation). In the case of the peak C_1 and C_2 of the CCA0 (Fig.5(a)), the reversible potentials are about 0.30 and 0.15 V vs. SHE, in very good agreement with the above Eqs. (1) and (3). Actually, since a buffer was not used, the approximate agreement is surprisingly good. Therefore, the peak C_1 is ascribed to the reduction of Cu^{2+} to Cu^+, and the peak C_2 is attributed to the reduction of Cu^{2+} to Cu^0 (the sum of Cu^{2+} to Cu^+ and Cu^+ to Cu^0). Correspondingly, the peak A_1 is due to the oxidation of Cu^0 to Cu^{2+}, and the peak A_2 corresponds to the oxidation of Cu^+ to Cu^{2+}. In addition, the same CV measurements of pure CeO_2 and CuO (prepared as the same process) were also carried out (Fig.5(f)). In the case of pure CeO_2, there is no peak in the cyclic voltammograms, whereas two large peaks appear in the case of pure CuO, indicating that the Ce^{4+}/Ce^{3+} redox couple does not exist in the potential range studied here.

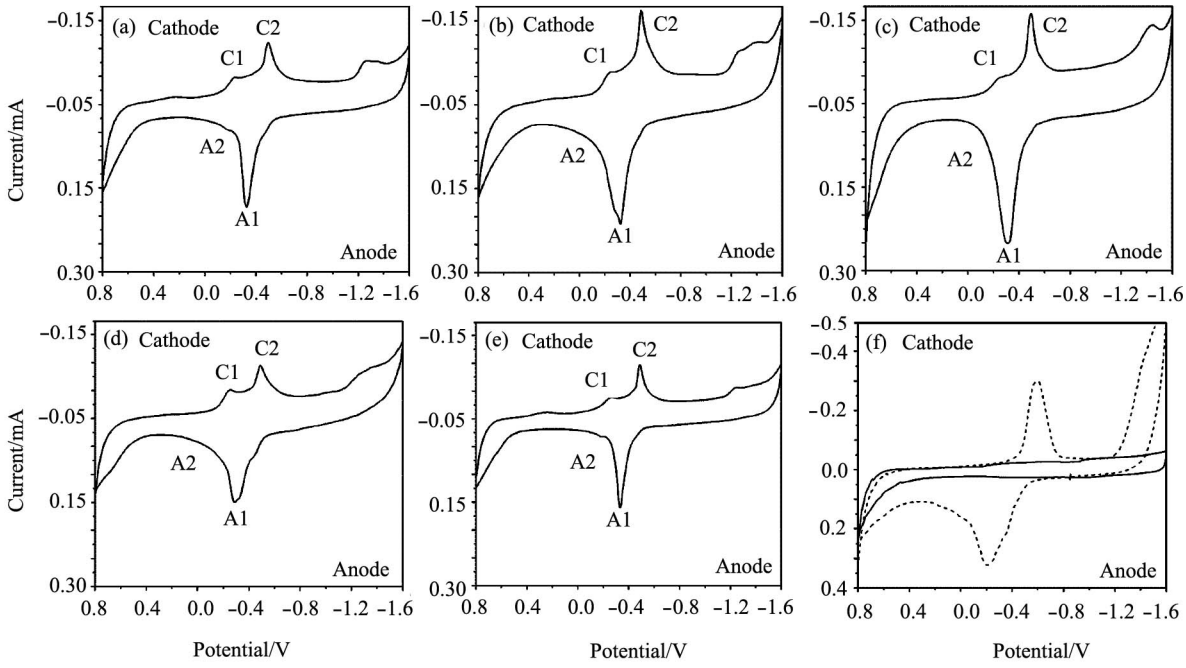

Fig.6 Cyclic voltammograms of copper species in yttrium doped CuO/CeO_2 catalysts in 0.05 mol/L Na_2SO_4 electrolyte at a scan rate of 10 mV/s
(a) CCY0; (b) CCY1; (c) CCY2; (d) CCY3; (e) CCY5; (f) Pure CeO_2 (solid line) and pure CuO (dot line)

The area of peak A_1 ($Cu^0 \rightarrow Cu^{2+}$) and C_2 ($Cu^{2+} \rightarrow Cu^0$), which represents the number of Cu^0(or Cu^{2+}) participating in the $Cu^0 \leftrightarrow Cu^{2+}$ reaction, reaches the maximum at CCY1 and CCY2, then falls off at CCY3 and CCY5 compared with CCY0. It is interesting to find that the variation of the redox peak area displays the same trend as that of catalytic activity, indicating that the number of Cu ions participating in the $Cu^0 \leftrightarrow Cu^{2+}$ reaction has great effect on the catalytic activity of WGS reaction in the present case.

On the other hand, the oxidative and reduction potentials for copper species in all cases are almost constant. Zhu et al.[28,29] reported that ΔE of catalyst is not an intrinsic factor in deciding the catalytic activity when there exists a reductive agent in the feed gas. We also consider that the ΔE of catalysts has less effect on the catalytic activity of WGS reaction, in which two reductive agents (CO and H_2) exist. Accordingly, ΔE of catalysts is not discussed in the present work.

3 Conclusion

CuO/CeO_2 catalysts doped with yttrium (0wt.%, 1wt.%, 2wt.%, 3wt.%, 5wt.%) prepared by co-precipitation were evaluated for WGS reaction in this work. A positive modification of structural and catalytic properties of CuO/CeO_2 had been achieved with certain amount of yttrium as dopant. The results indicated that as yttrium doping was 2wt.%, the catalyst had the largest surface area and showed the highest catalytic activity and thermal stability. The WGS activity was correlated well with the variation of surface area, the area of the reductive peak γ (i.e., the reduction of surface copper oxide (crystalline forms) interacted with surface oxygen vacancies on ceria) and the area of peak C_2 and A_1 ($Cu^0 \leftrightarrow Cu^{2+}$ in cyclic voltammetry process), thus it was concluded that the interaction between copper species and surface oxygen vacancies on ceria played a decisive role in the WGS reaction. Furthermore, considering their high catalytic performance and low cost, it could suggest the potential industrial applicability of co-precipitation synthesized Y-doped CuO/CeO_2 catalysts in WGS reaction.

References:

[1] Trimm D L. Minimization of carbon monoxide in a hydrogen stream for fuel cell application. *Appl. Catal. A*, 2005, **296**(1): 1.
[2] Swartz S L, Seabaugh M M, Holt C T, Dawson W J. Fuel processing catalysts based on nanoscale ceria. *Fuel cells Bulletin*, 2001, **4**(30): 7.
[3] Fu Q, Weber A, Flytzani-Stephanopoulos M. Nanostructured Au-CeO_2 catalysts for low-temperature water-gas shift reaction. *Catal. Lett.*, 2001, **77**: 87.
[4] Idakiev V, Yuan Z Y, Tabakova T, Su B L. Titanium oxide nanotubes as supports of nano-sized gold catalysts for low temperature water-gas shift reaction. *Appl. Catal. A*, 2005, **281**: 149.
[5] Zhang F L, Zheng Q, Wei K M, Lin X Y, Zhang Y Y, Li J W,

Cao Y N. Improved performance of Au/Fe_2O_3 catalysts promoted with ZrO_2 and Nb_2O_5 in the WGS reaction. *Catal. Lett.*, 2006, **108**: 131.

[6] Wang X, Gorte R J, Wagner J P. Deactivation mechanisms for Pd/Ceria during the water-gas-shift reaction. *J. Catal.*, 2002, **212**: 225.

[7] He R, Davda R R, Dumesic J A. In situ ATR-IR spectroscopic and reaction kinetics studies of water-gas shift and methanol reforming on Pt/Al_2O_3 catalysts in vapor and liquid phases. *J. Phys. Chem. B*, 2005, **109**: 2810.

[8] Jacobs G, Williams L, Graham U, Sparks D, Davis B H. Low-temperature water-gas shift: In-situ DRIFTS-reaction study of a Pt/CeO_2 catalyst for fuel cell system. *J. Phys. Chem. B*, 2003, **107**: 10398.

[9] Basinska A, Domka F. The influence of alkali metals on the activity of supported ruthenium catalysts for the water-gas shift reaction. *Catal. Lett.*, 1997, **43**: 59.

[10] Li Y, Fu Q, Flytzani-Stephanopoulos M. Low-temperature water-gas shift reaction over Cu- and Ni-loaded cerium oxide catalysts. *Appl. Catal. B*, 2000, **27**: 179.

[11] Tabakova T, Idakiev V, Papavasiliou J, Avgouroupoulos G, Ioannides T. Effect of additives on the WGS activity of combustion synthesized CuO/CeO_2 catalysts. *Catal. Commun.*, 2007, **8**: 101.

[12] Qi X M, Flytzani-Stephanopoulos M. Activity and stability of $Cu\text{-}CeO_2$ catalysts in high-temperature water-gas shift for fuel-cell application. *Ind. Eng. Chem. Res.*, 2004, **43**: 3055.

[13] Montross C S. Precipitation and bulk property behavior in the yttria-magnesia-zirconia ternary system. *Br. Ceram. Trans. J.*, 1991, **90**: 175.

[14] Rajiv D, Richards V L, Wang X P. Development of ceria-based electrelytes. *J. Electrochem. Soc.*, 1998, **145**(2): 414.

[15] Song X L, Jiang N, Li Y K, Xu D Y, Qiu G Z. Synthesis and characterization of Y-doped mesoporous CeO_2 using a chemical precipitation method. *Journal of Rare Earths*, 2007, **25**: 428.

[16] Petot G. E, Zientara C P D, Kusinski J. Microstructure and transport properties of Y-doped zirconia and Gd-doped ceria. *Material Chemistry and Physics*, 2003, **81**: 305.

[17] Ramrez E C, Atkinson A, Chadwick D. Reactivity of ceria, Gd- and Nb-doped ceria to methane. *Appl. Catal. B*, 2002, **36**: 193.

[18] Nitani H, Nakagawa N, Yamanouchi M, Osuki T, Yuya M, Yamamoto T A. XAFS and XRD study of ceria doped with Pr, Nd or Sm. *Materials Letters*, 2004, **58**: 2076.

[19] Xie Y C, Tang Y Q. Spontaneous Monolayer Dispersion of oxides and salts onto surfaces of supports: applications to heterogereous catolysis. *Advances in Catalysis*, 1990, **37**: 1.

[20] Chen Y, Zhang L F. Surface interaction model of γ-alumina-supported metal oxides. *Catalysis Letters*, 1992, **12**: 51.

[21] Shan W S, Feng Z C, Li Z L, Zhang J, Shen W J, Li C. Oxidative steam reforming of methanol on $Ce_{0.9}Cu_{0.1}O_r$ catalysts prepared by deposition-precipitation, coprecipitation, and complexation-combustion methods. *Journal of Catalysis*, 2004, **228**: 206.

[22] McBride J R, Hass K C, Poindexter B D, Weber W H. Raman and X-ray studies $Ce_{1-x}RE_xO_{2-\delta}$, where RE=La, Pr, Nd, Eu, Gd, and Tb. *J. Appl. Phys.*, 1994, **76**: 2435.

[23] Yao C Z, Wang L C, Liu Y M, Wu G S, Cao Y, Dai W L, He H Y, Fan K N. Effect of preparation method on the hydrogen production from methanol steam reforming over binary Cu/ZrO_2 catalysts. *Applied Catalysis A*, 2006, **297**: 151.

[24] Zheng X C, Zhang X L, Wang X Y, Wang S R, Wu S H. Preparation and characterization of CuO/CeO_2 catalysts and their applications in low-temperature CO oxidation. *Applied Catalysis A*, 2005, **295**: 142.

[25] Tang X L, Zhang B C, Li Y, Xu Y D, Xin Q, Shen W J. Carbon monoxide oxidation over CuO/CeO_2 catalysts. *Catal. Today*, 2004, **93-95**: 191.

[26] George A, Theophilos I. Selective CO oxidation over $CuO\text{-}CeO_2$ catalysts prepared via the urea-nitrate combustion method. *Applied Catalysis A*, 2003, **224**: 155.

[27] Bera P, Mitra S, Sampath S, Hegde M S. Promoting Effect of CeO_2 in a Cu/CeO_2 catalyst: lowering of redox potential of Cu species in the CeO_2 matrix. *Chem. Commun.*, 2001, (10): 927.

[28] Zhu J, Zhao Z, Xiao D, Li J, Yang X, Wu Y. Application of cyclic voltammetry in heterogeneous catalysis: NO decomposition and reduction. *Electrochemistry Communications*, 2005, **7**: 58.

[29] Zhu J, Zhao Z, Xiao D, Li J, Yang X, Wu Y. Study of $La_{2-x}Sr_xCuO_4$ (x = 0.0, 0.5, 1.0) catalysts for NO+CO reaction from the measurements of O_2-TPD, H_2-TPR and cyclic voltammetry. *J. Mol. Catal. A: Chem.*, 2005, **238**: 35.